Genetic analysis of crawling and swimming locomotory patterns in *C. elegans*

Jonathan T. Pierce-Shimomura[a,1], Beth L. Chen[b], James J. Mun[a], Raymond Ho[a], Raman Sarkis[a], and Steven L. McIntire[a,2]

[a]Ernest Gallo Clinic and Research Center, Department of Neurology, Programs in Neuroscience and Biomedical Science, University of California, San Francisco, Emeryville, CA 94608; and [b]Cold Spring Harbor Laboratory, Cold Spring Harbor, NY 11724

Communicated by Cornelia Bargmann, Rockefeller University, New York, NY, October 15, 2008 (received for review April 19, 2008)

Alternative patterns of neural activity drive different rhythmic locomotory patterns in both invertebrates and mammals. The neuro-molecular mechanisms responsible for the expression of rhythmic behavioral patterns are poorly understood. Here we show that *Caenorhabditis elegans* switches between distinct forms of locomotion, or crawling versus swimming, when transitioning between solid and liquid environments. These forms of locomotion are distinguished by distinct kinematics and different underlying patterns of neuromuscular activity, as determined by *in vivo* calcium imaging. The expression of swimming versus crawling rhythms is regulated by sensory input. In a screen for mutants that are defective in transitioning between crawl and swim behavior, we identified *unc-79* and *unc-80*, two mutants known to be defective in NCA ion channel stabilization. Genetic and behavioral analyses suggest that the NCA channels enable the transition to rapid rhythmic behaviors in *C. elegans*. *unc-79*, *unc-80*, and the NCA channels represent a conserved set of genes critical for behavioral pattern generation.

neural rhythms | neurogenetics | sodium leak channel

Different forms of rhythmic neural output are ubiquitously observed in motor behaviors such as locomotion, respiration, and feeding (1–4). Extensive research has revealed that a neural network can switch among alternate rhythms by altering the properties of specific intrinsic membrane currents and synapses (5). Consistent with this framework, some proteins appear to contribute more to the generation of one rhythm than other rhythms. For instance, channels that carry the persistent sodium current appear to be important for gasping but not the normal respiratory rhythm when studied *in vitro* (6). Physiological approaches are sometimes limited when trying to identify specific proteins involved in certain rhythms, however, because of the availability and selectivity of compounds that act on the relevant molecules. With the advent of reverse genetics, these limitations are beginning to be overcome by knocking out or modifying specific genes (7, 8), but both pharmacological and gene manipulation approaches are still limited by the *a priori* hypotheses on which molecules to target. In contrast, because forward genetic studies are unbiased, they can lead to the identification of novel or uncharacterized proteins that contribute to rhythmic neural output. We have therefore pursued a forward genetic approach to identify neural proteins that contribute more to the generation of one form of rhythmic locomotion (i.e., swimming) than another (i.e., crawling) in the nematode *Caenorhabditis elegans*.

C. elegans moves by generating waves of dorsal-ventral (DV) bends along its body. Prior genetic studies have focused on the molecular mechanisms responsible for crawling over a solid agar substrate (9, 10), whereas the motion *C. elegans* displays in liquid has only begun to be characterized (11). Although *C. elegans* encounters water in its natural environment (12), it has been unclear whether its motion in liquid (previously called "thrashing") contributes to a directed form of locomotion better described as "swimming" and whether this form of motion is generated by neuromuscular activities distinct from crawling. Here we show that swimming is distinct from crawling in both kinematics and pattern of muscle activity. Furthermore, we have begun to genetically define the molecular mechanisms responsible for the generation of crawling and swimming. We provide evidence from analysis of sensory mutants that maintenance of swimming, rather than crawl-like behavior in liquid, requires sensory input. We then performed a genetic screen to identify a set of molecules from a recently described putative nematode cation channel (NCA) (13–16) that is crucial for the swimming form of locomotion.

Results

Crawling and Swimming Are Characterized by Unique Kinematics. To compare crawl and swim forms of locomotion in WT animals, we video-recorded individual worms first as they crawled across an agar surface, and second as they swam in liquid [supporting information (SI) Movies S1 and S2]. A time-series of five animal postures from a complete cycle of crawling and swimming for a representative individual is shown in Fig. 1*A*. *C. elegans* lie on either their left or right side while DV bends propagate along the anterior-posterior axis forming distinctive postures. Crawling is characterized by a persistent S-shaped posture whereas swimming is usually characterized by a C-shaped posture.

We quantified the curvature of the animal's midline during crawling and swimming to test whether these forms of motion differ not only in the frequency of bending, but also in how the posture changes over time. Curvature analysis highlighted key differences in crawl and swim kinematics. For crawling, the worm's head completes a full cycle of DV bending before a single bend propagates from head to tail, whereas for swimming, the bend propagates within the amount of time the head completes the DV cycle (Fig. 1*B*). Plots of the curvature of the second most anterior midline angle (i.e., "neck") also reveal that crawl bends were deeper and slower in frequency than swim bends (Fig. 1 *C* and *D*). To quantify the common frequencies of bending during crawl and swim, we performed a power spectrum analysis of the neck curvature (Fig. 1*D*). A single peak in bend frequencies was observed at ≈0.8 Hz for crawl and at ≈2.1 Hz for swim. Thus, swimming is not merely a faster version of crawling; rather, crawl and swim have kinematics that are quantitatively distinct in frequency, amplitude, and propagation of DV bends.

Swimming Is a Directed Form of Locomotion for *C. elegans*. Prior studies have referred to *C. elegans* motion in liquid as an undirected thrashing. We hypothesized that *C. elegans* may instead use swimming to direct its motion in an attractive

Author contributions: J.T.P.-S. and S.L.M. designed research; J.T.P.-S., B.L.C., J.J.M., R.H., and R.S. performed research; J.T.P.-S. and B.L.C. contributed new reagents/analytic tools; J.T.P.-S. and B.L.C. analyzed data; and J.T.P.-S. and S.L.M. wrote the paper.

The authors declare no conflict of interest.

[1]Present address: Section of Neurobiology, University of Texas, Austin, TX 78712.

[2]To whom correspondence should be addressed. E-mail: slm@gallo.ucsf.edu.

This article contains supporting information online at www.pnas.org/cgi/content/full/0810359105/DCSupplemental.

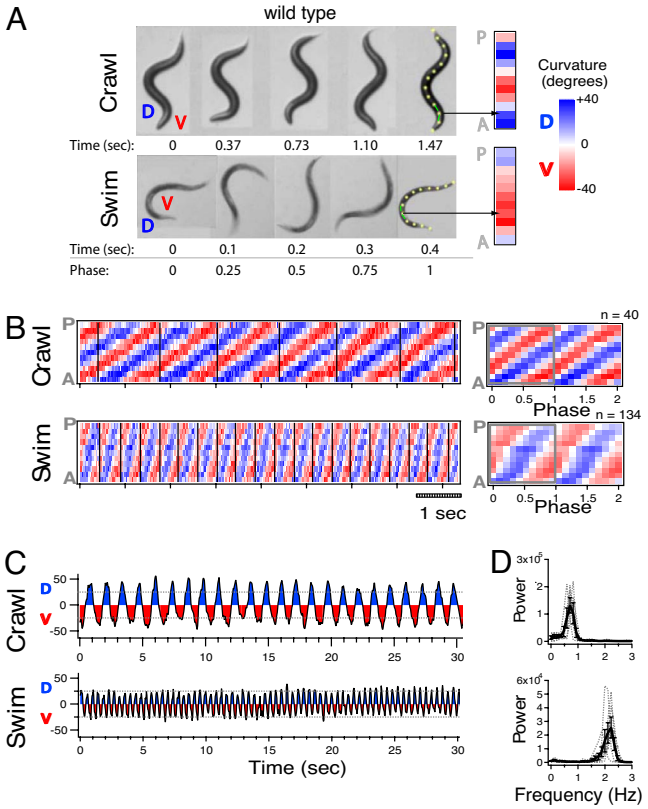

Fig. 1. Crawling and swimming are characterized by distinct kinematics. (*A*) Video frames of the same WT animal crawling and swimming. Time and phase of the DV head-bend cycle are indicated below each frame. DV cycle start is defined as the moment the head turns dorsal. Note that the body always forms a C-like shape immediately before this turn. Curvature columns (*Right*) represent curvature for each of the 11 angles along the example midlines aligned anterior to posterior (A, P). Example angles are matched by arrows. (*B*) Crawl and swim curvature matrices for a WT individual. Average curvature matrix for DV head-bend cycles are shown (*Right*) with number of averaged cycles indicated above. (*C*) Plots of neck curvature versus time for the same individual. Plots of average power versus frequency of neck curvature across individuals (*D*). Individual traces are indicated by gray lines. Bars represent SEM.

gradient. A droplet containing a group of animals was placed on a smooth, level field of agar that contained a gradient of sodium chloride (Fig. 2*A*). Within seconds, animals accumulated on the attractive side (at 10 sec, 74% ± 4%; $t_9 = 8.35$, $P < 0.0001$; Fig.

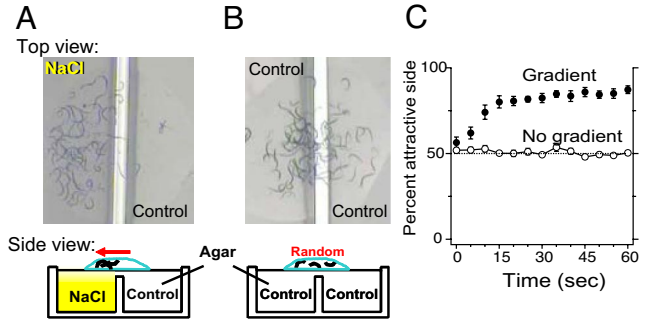

Fig. 2. Swimming as a directed form of locomotion for *C. elegans*. Photos of groups of WT animals swimming in a puddle dropped over agar containing either a salt gradient (*A*) or no gradient (*B*). Cross-section layout of the agar assay plates and liquid drops below. (*C*) Average percent of individuals on attractive side versus time for animals in gradient or control assays. Bars represent SEM.

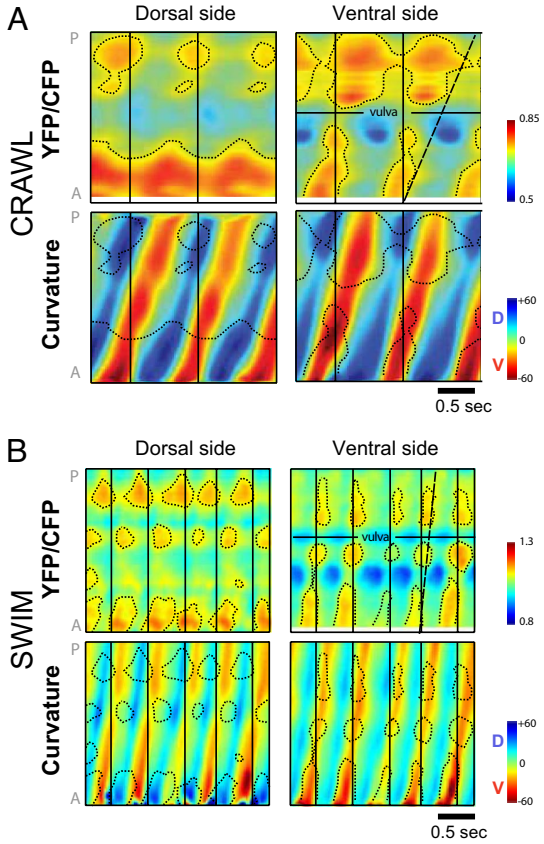

Fig. 3. Crawling and swimming are generated by distinct patterns of muscle activity. (*A* and *B*) Muscle activity of opposing dorsal and ventral muscle quadrants in a crawling (*A*) and swimming (*B*) animals. Plots of intensity ratio (YFP/CFP) for cameleon in body-wall muscle along anterior-posterior axis versus time shown above. Corresponding curvature matrices for dorsal and ventral body sides shown below. Note that areas of peak muscle activity (contour lines) for dorsal side generally coincide with or slightly precede corresponding areas of dorsal curvature (green/blue) whereas areas of peak muscle activity for ventral side coincide with or slightly precede corresponding areas of ventral curvature (yellow/red). Positions on anteroposterior axis with no observed ratio change are a result of absence of expression of cameleon extra-chromosomal array. Color key for intensity ratio is shown (*Right*). Vertical black lines distinguish head bend cycles. Slanted/dashed lines correspond to end of one cycle of ventral muscle activity and highlight the rapid propagation of ventral muscle activity for swimming versus crawling with respect to DV head bending. Color key for body-side curvature matrices uses blue-green-yellow-red color scheme to contrast with body-midline curvature matrices, which use blue-white-red color scheme in other figures.

2*C*) while separate groups of control animals swam randomly (Fig. 2 *B* and *C*). Therefore, *C. elegans* can use swimming as an efficient way to "chemotax" in liquid, which may be important in its natural environment.

Distinct Muscle Activation Patterns Underlie Crawling and Swimming. From simple observation of *C. elegans*, one cannot firmly distinguish between differences in motion caused by forces exerted by the muscles versus motion caused by reactionary elastic and frictional forces. To address this issue, we looked directly at muscle activity in individual unrestrained crawling and swimming worms by recording calcium transients in body wall muscles of whole animals using cameleon.

Our imaging results demonstrate that crawling and swimming are generated by distinct patterns of muscle activity. Fig. 3 *A* and *B* show representative muscle activity with the corresponding curvature per body side for both crawling and swimming worms,

NEUROSCIENCE

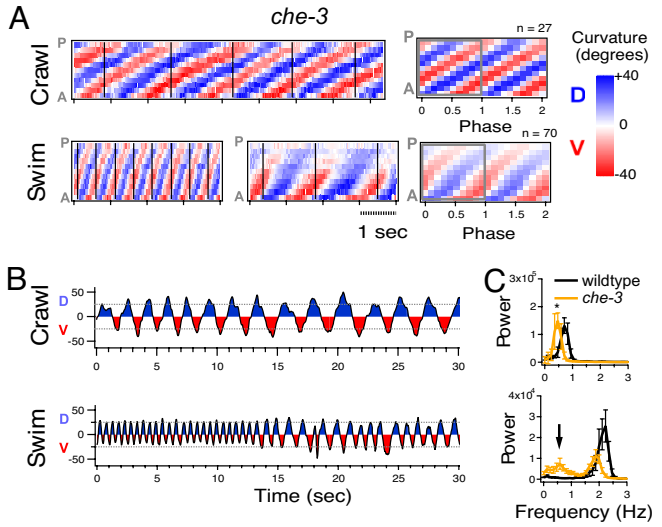

Fig. 4. Sensory regulation of the expression of crawling and swimming. (*A*) Crawl and swim curvature matrices for a *che-3* mutant. Two panels are shown for "Swim" to demonstrate switch between nearly normal swimming (*Left*) and crawl-like motion (*Right*). Average curvature matrix for DV head-bend cycles are shown (*Right*). (*B*) Plots of neck curvature versus time for the same individual. Example of swim curvature demonstrates a switch from normal swim to crawl-like motion even though the animal remains in liquid. (*C*) Plots of average power versus frequency of neck curvature across individuals. $*P <$ 0.05 with Tukey test of multiple comparison. Arrowhead indicates extra peak in the *che-3* mutant distribution. Bars represent SEM.

respectively. The body-side curvature matrices (*Bottom*, Fig. 3 *A* and *B*) are similar to midline-curvature matrices obtained by video alone in frequency and pattern of waveform propagation (Fig. 1*B*). The different patterns of activation of opposing dorsal and ventral muscles (dotted areas, *Top*, Fig. 3 *A* and *B*) precede or coincide with the different patterns of body bending to the dorsal and ventral sides (corresponding dotted areas, *Bottom*, Fig. 3 *A* and *B*). The distinct patterns of muscle activity for crawl and swim are especially apparent when comparing ventral muscle activity. Consistent with the different kinematics in Fig. 1, ventral muscle activity propagates backward much faster for swimming than crawling with respect to the DV head bending (compare dashed lines in Fig. 3*A* vs. Fig. 3*B*). Hence, body bends reflect muscle activity, and the different patterns of body bending for swim and crawl are produced primarily by distinct patterns of contractions of the body muscles.

Sensory Neurons Regulate the Expression of Swimming Versus Crawling. We tested whether sensory input influences the selection of a crawl versus swim motor pattern by examining the *che-3* mutant. This mutant is defective in the development of all ciliated sensory neurons (17). We found that *che-3* mutants crawled with normal amplitude and propagation of DV bends, but displayed a slightly lower frequency of bending (Fig. 4 *A–C*; Movie S3). By contrast, in liquid, *che-3* mutants displayed periods of normal swim behavior in alternation with periods of crawl-like behavior (Fig. 4 *A–C* and Movie S4). The change between the two locomotory patterns was abrupt, such that the entire animal moved with either a swim or crawl-like pattern and not with a mixture of the two patterns. A curvature matrix from a representative individual is shown in Fig. 4*A* and the corresponding neck curvature is shown in Fig. 4*B*. At first, the animal moved with normal swim frequency and amplitude, but later switched to a crawl-like frequency, amplitude, and pattern of propagation. Crawl-like kinematics were reflected in an average curvature matrix for this *che-3* individual that clearly resembled a WT crawl matrix rather than a WT swim matrix (Fig. 1*B* and Fig. 4*A*). This phenotype was also reflected in a bimodal distribution in the average bend frequency histogram. One peak aligned with the peak crawl frequency for *che-3*, and a second peak aligned near the peak swim frequency for WT (Fig. 4*C*). Analysis of mutants with defects in different subsets of ciliated sensory neurons revealed less severe defects in swim behavior than *che-3* (Fig. S1). These mutants often displayed a pattern of motion that appeared to be a mixture between normal swim and crawl-like patterns. For example, the *osm-3* mutant displays a normal swim frequency but a crawl-like amplitude in liquid (Fig. S1). Assuming that *che-3* and *osm-3* function solely in sensory neurons, our results suggest that the correct expression of the appropriate motor program in *C. elegans* depends on inputs from multiple ciliated sensory neurons.

The observation that sensory mutants can move with crawl-like motion in liquid prompted us to reinvestigate whether WT worms could ever exhibit the same behavior. Although WT animals always moved with C-shaped kinematics during the first minute while swimming, rare transient bouts of crawl-like behavior can sometimes be observed after WT animals have been in liquid for extended periods (60–75 min; Fig. S2). This is consistent with the conclusion that the physical forces impinging on the animal by the liquid environment do not dictate the usual C-shaped kinematics generally observed in WT swimming.

Genetic Screen for Mutants Defective in Transitioning from Crawl to Swim. If crawling and swimming are controlled by distinct patterns of neuromuscular activity, there may be other genes that are preferentially involved in swimming, and/or in the transition between crawl and swim. Therefore, we completed a genetic screen for mutants capable of normal crawling but incapable of normal swimming. We found more than 40 mutants that exhibited little or no defect in crawling, but showed a grossly abnormal pattern of swim activity (*Swim abnormal* [Swa] phenotype). Each Swa mutant could be classified by the type of swim defect; however, we found only one Swa mutant class that became paralyzed upon immersion in liquid. All three mutants in this class shared a potentially related "fainter" phenotype when crawling. Fainter mutants crawl well for long distances but inexplicably stop or "faint," remaining immobile for a period before re-initiating movement (18). Fainting was robustly elicited during crawling escape responses to mechanical stimulation and always occurred after spontaneous attempts at backward crawling. Two of these alleles corresponded to *unc-79*, whereas the third corresponded to *unc-80*. We did not detect any gross abnormality in neuronal cell body position, neuronal processes, or fasciculation in these strains (data not shown), suggesting that these mutations do not interfere with nervous system development.

Both *unc-79* and *unc-80* were recently cloned and found to encode large novel proteins with a single orthologues conserved in flies and mammals (13, 15) (Fig. S3*C*). We obtained transformation rescue of the *unc-80* locomotion phenotypes with the predicted *unc-80* ORF and 2.7-kb promoter region (Fig. 5 *D* and *E*). Analysis for potential motifs revealed that UNC-79 and UNC-80 predicted proteins share a central armadillo motif that may be important in protein-protein binding interactions (Fig. S3*C*) (19, 20). We compared the expression pattern of *unc-79* with *unc-80* by expressing GFP driven by 2.7-kb promoter regions for each gene. Fluorescence patterns overlapped throughout the nervous system (Fig. S3*D*), suggesting that UNC-79 and UNC-80 proteins may function together in the same neurons.

We quantitatively compared the crawling and swimming of fainter mutants with that of WT animals. Both *unc-79* and *unc-80* single mutants, as well as the *unc-79;unc-80* double mutant, displayed identical phenotypes. Fainter mutants crawled forward with a slightly slower frequency, amplitude, and propagation of

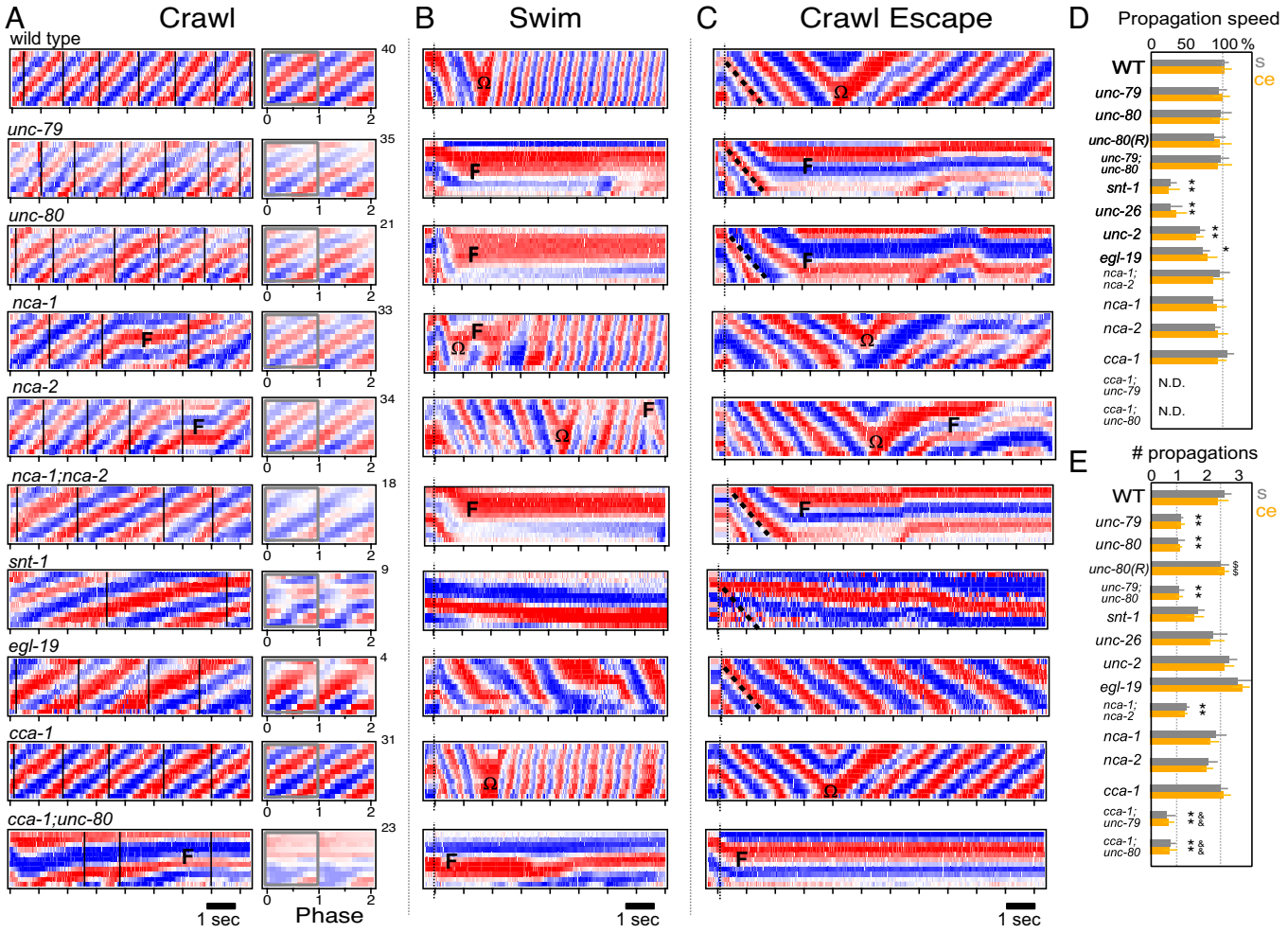

Fig. 5. Comparison of WT and mutant patterns of locomotion. (*A*) On crawling curvature matrices, vertical lines distinguish DV head-bend cycles. Corresponding average DV cycle curvature matrix is shown (*Right*). Number of averaged cycles indicated above. (*B*) Swimming curvature matrices: dotted vertical lines indicates when animals entered liquid. (*C*) Crawl escape curvature matrices: dotted vertical lines indicates stimulation time. (*D*) Average propagation speed of first DV bend for swimming (s; gray) and crawl escape (ce; orange) relative to WT (s, 0.85 sec^{-1}; ce, 1.75 sec^{-1}). Speed not calculated for *cca-1* double mutants (N. D.) because of incomplete bend propagation. (*E*) Average number of DV bends propagated for initial swimming and crawl escape motion before omega bend (Ω) or faint episode (F). Rescue strain *unc-80*;*Punc-80*(+) indicated by *unc-80*(*R*). Symbols show differences (*) from WT, ($) from *unc-80*, or (&) from *nca-1*;*nca-2*; $P < 0.05$. $n = 15$ for each bar. Bars represent SEM with Tukey test of multiple comparison.

bends compared with WT animals, but with an otherwise well coordinated waveform reflected in curvature matrices that resembled muted versions of the WT matrix (Fig. 5*A* and Movie S5). Whereas WT animals moved continuously upon immersion, fainter mutants ceased movement in less than 1 sec after a single DV bend was passed from tail to head (Fig. 5 *B* and *F* and Movies S2 and S6). The speed and pattern of the single propagated DV bend was normal (Fig. 5 *B* and *D*). During the immobile state, animals maintained a fixed posture from several seconds to more than 30 seconds (Fig. 5*B*). Fainter mutants never generated a normal pattern of swimming and frequently repeated the immobile behavior described earlier.

The fainter phenotype has been attributed to lack of a novel class of NCA-type ion channel because the *nca-1*;*nca-2* double mutant shares the fainter phenotype and *unc-79* and *unc-80* mutants have undetectable levels of NCA-1 and NCA-2 ion channels (16). The mammalian NCA channel orthologue (NALCN) has recently been functionally characterized as a sodium "leak" channel that acts to raise resting potential greater than the equilibrium potential for potassium (14). We found that the reported expression patterns of *nca-1* and *nca-2* genes overlap with our expression patterns for both *unc-79* and *unc-80* genes in the cholinergic motor neurons in the nerve cord. We also found that the *nca-1*;*nca-2* double mutant is capable of crawling for long periods (Fig. 5*A*), but faints during swimming and crawl escape responses (Fig. 5 *B* and *C*). Previously, the *nca-1* and *nca-2* single mutants were reported to display normal crawling (13). We found, however, that both mutants displayed short-duration fainting episodes during crawling and swimming (Fig. 5 *A* and *B*). These data suggest that *unc-79*, *unc-80*, *nca-1*, and *nca-2* function together (i.e., "NCA pathway") to regulate the transition from slow to rapid forms of locomotion.

The rapid paralytic response exhibited by the NCA pathway mutants in liquid was remarkable given that even major synaptic and calcium channel mutants that are all severely defective in crawling move immediately and repetitively upon immersion in liquid (e.g., synaptotagmin *snt-1*, synaptojanin *unc-26*, and voltage-gated calcium channel mutants *unc-2* (i.e., P/Q type) and *egl-19* (i.e., L type; Fig. 5*B*) (21–23). Individuals from each mutant group displayed defective swimming, characterized by various degrees of slow bend frequency and irregular waveform, but they still passed multiple complete DV bends along the body in liquid (Fig. 5 *B*, *D*, and *E*). This defect is opposite in character to *unc-79* and *unc-80*, in which a single waveform propagates

with normal speed and coordination, but no recognizable swimming rhythm is established. Together these results suggest that the fainter phenotype cannot be explained by a general defect in synaptic function or neuron excitability.

We next sought to determine whether there is a relationship between fainting while swimming and fainting while crawling. Upon mechanical stimulation to the head, WT animals rapidly reverse direction. WT animals invariably propagated multiple bends along their body before usually (80% of the time; $n = 30$) turning with a ventral omega-shaped bend to move away from the stimulus (Fig. 5 *C–E*). By contrast, fainter mutants move backward normally by passing exactly one DV bend from tail to head before abruptly stopping (Fig. 5 *C–E*). Several crawl-defective mutants displayed escape responses similar to WT in that they also passed multiple DV bends (albeit slowly) along the body and often completed an omega bend (Fig. 5 *C–E*). Thus, for both crawl and swim fainter phenotypes, NCA pathway mutants freeze their posture after a single DV bend propagates rapidly along the body in an attempt to switch from a slower to a faster form of locomotion.

How does the initial DV body bend propagate during rapid locomotion in the absence of the NCA pathway? Rapid initiation of rhythmic pumping of the *C. elegans* pharyngeal muscle relies on the transient T-type calcium channel (24). We hypothesized that the initial rapid propagation of a DV bend may similarly depend on the T-type calcium channel CCA-1 in NCA pathway mutants. Consistent with this hypothesis, we found that, although *cca-1* single mutants displayed normal swimming (Fig. 5*B*), *cca-1*;*unc-79* and *cca-1*;*unc-80* double mutants showed spontaneous faint-like behavior after a DV bend propagated only one fourth to one half of the body length during attempts at swimming and escape crawling (Fig. 5 *B* and *C*). These data suggest that the NCA and T-type channels are functionally redundant for initiating rapid forms of locomotion.

Last, we noticed that, although *cca-1* single mutants displayed well coordinated crawling with only slightly deeper bends and slower frequency in comparison with WT (Fig. 5*A*), *cca-1*;*unc-79* and *cca-1*;*unc-80* double mutant animals displayed a severe defect in crawling that was not shared with either of the single mutant parent strains (Fig. 5*A*). The defective crawling resembled repeated episodes of faint-like behavior described earlier whereby the mutants never propagated a DV bend along the whole body length. Overall, these results support a model in which the T-type channel enables propagation of DV bends for both slow (i.e., crawling) and rapid (i.e., swimming) forms of locomotion in the absence of NCA-type channel function.

Discussion

Through kinematic analysis, we have found that *C. elegans* has two fundamental forms of locomotion: crawling and swimming. The observation that worms can move robustly toward an attractant even while submersed in liquid suggests that *C. elegans* may have adapted to prosper in wet environments such as in a damp soil matrix or associated with carrier species such as snails (12). Because *C. elegans* lives near the liquid/air interface, it may have adapted mechanisms to rapidly switch between distinct kinematics for efficient locomotion in both conditions.

C. elegans experiences a range of different physical forces in dry versus liquid environments. We propose that the animal senses some of these forces to "decide" to move with a certain pattern, whereas some forces passively constrain the pattern of movement regardless of whether the animal can sense them. Our calcium imaging results indicate that, despite these differences in environmental forces, the pattern of muscle activity can explain the S- and C-shaped body kinematics displayed in crawling and swimming.

Studying crawl and swim forms of locomotion in *C. elegans* addresses how transitions between different rhythmic patterns are mediated by the nervous system. An analogous approach of studying the choice between crawling and swimming in the leech has proven useful to understand how identified neurons participate in this complex task *in vitro* (25, 26). In *C. elegans* we can study the genetic regulation of the crawl/swim choice *in vivo*. Unlike in WT animals, the gross sensory mutant *che-3* displayed abrupt switching between bouts of swim and crawl-like motion in liquid. The discontinuous nature of the locomotory phenotype lends support to the idea that crawl and swim forms of locomotion represent discrete behaviors rather than a single behavior in which the kinematics change in a continuous manner. Future studies will elucidate how different sensory pathways contribute to the normal expression of the swimming pattern.

The NCA-deficient mutants were the only mutants from our screen that displayed transient paralysis after immersion in liquid. The paralytic defect in swimming displayed by NCA-deficient mutants cannot be explained by general defects in neuronal excitability, synaptic function, or development because the fainting phenotype was not observed in mutants defective in voltage-gated calcium channels or major synaptic proteins. Instead, the conserved genes that comprise the NCA pathway (*unc-79*, *unc-80*, and *nca*-type) represent a key set of molecules that function in the transition to rapid neuromuscular rhythms.

Only recently has the identity and role of the NCA-type sodium "leak" channel (i.e., NALCN) been described in mammals (14). Interestingly, NALCN-KO mice show no obvious defect in neuronal development, but die shortly after birth as a result of an abnormal respiratory rhythm (14). *unc-79*-KO mice also display post-embryonic lethality without obvious developmental defects (27). The *Drosophila* NCA-type channel mutant *na* is reported to walk with faint-like "hesitations" (13). Although we cannot rule out roles for the NCA pathway in subtle aspects of development, data among laboratories suggest a conserved role in the generation of rhythmic behaviors.

UNC-79 and UNC-80 were recently found necessary for stability of NCA-type channels in *C. elegans* and in *Drosophila* species (13, 15, 16). mRNA of the *unc-80* orthologue is reported to be enriched in neural tissue in both mouse and human (28, 29). Our promoter analysis suggests that *unc-79* and *unc-80* are co-expressed in neurons, consistent with the overlapping neural expression of their mouse orthologues (28). UNC-79 was also found to stabilize expression of UNC-80 and vice versa in *C. elegans* (16). Thus, UNC-79 and UNC-80 might function together in the nervous system in mammals as well as in invertebrates.

The T-type calcium channel appears to have both singular and synergistic roles in crawling. By itself, the T-type channel is required for normal bend amplitude and frequency. More importantly, in combination with the NCA-type channels, the T-type channel is crucial to maintain DV bend propagation in crawling. Although it is currently unclear how the T-type channel achieves these roles, we speculate that the roles for the T-type channel in crawling and swimming may be attributed to its fast inactivation ($\approx$10 to 50 ms) and slow recovery ($\approx$400 ms) kinetics (24, 30). This combination might make it well "tuned" to participate as a rebound current in ventral cord motor neurons to sustain slow rhythmic locomotion (crawl quarter cycle $\approx$625 ms), but perhaps preclude it from recovering in time to participate significantly in sustaining rapid rhythmic locomotion (quarter cycles for crawl escape $\approx$250 ms and swim $\approx$100 ms). By contrast, NCA-type channels, which do not inactivate (14), may work synergistically in motor neurons with the T-type channel during slow rhythmic behavior, but then take a leading role in the rebound potential during rapid rhythmic behaviors. Although "leak" currents are not typically thought of as "rebound" currents, they can contribute significantly to rebound membrane potential of rhythmic neurons and muscles following hyperpolarization (31, 32). Therefore, NCA-type and T-type channels

may also work together to sustain specific rhythmic patterns in higher organisms.

Materials and Methods

Video Analysis. Individual young adult *C. elegans* were video-recorded blind to genotype (1 min, 30 frames/sec, 344 pixels/mm) as they moved over nematode growth medium (NGM) agar plate (6-cm diameter) covered with (i.e., swim) or without (i.e., crawl) 3 ml NGM buffer. For escape crawl condition, a worm was transferred to an NGM plate and recorded while prodded quickly on the side of the head with a platinum wire. Animal midlines (13 points) were derived with a custom image analysis algorithm (ImagePro; Media Cybernetics). The series of 11 angles formed by the midline was represented in a color-coded ''curvature column'' (Fig. 1*A*). A time series of curvature columns formed a ''curvature matrix'' (e.g., Fig. 1*B*) in which blue and red stripes represent the waves of dorsal and ventral curvature, respectively, passing along the body. Curvature matrices were divided into head-bend cycles based on curvature of the most anterior row in the curvature matrix. Curvature column values were divided into 10 bins evenly distributed across each DV cycle to average across DV cycles weighted by duration (e.g., Fig. 1*B*, *Right*). Power spectrum of ''neck'' curvature was analyzed with IgorPro (Wave Metrics). Chemotaxis in liquid assay and specific strains are described in *SI Materials and Methods*.

Muscle Imaging. To image calcium transients in muscles of unrestrained moving worms, we used the strain *kyEx302*, which harbored an extra-chromosomal array expressing YC2 under the *myo-3* promoter specific to muscles (see *SI Materials and Methods*).

Swim-Abnormal Screen. Swa mutants were obtained by placing the F2 progeny of EMS-mutagenized worms on one side of an NGM agar plate (6-cm diameter). Individuals that crawled to bacteria on the opposite side within 20 min were transferred to NGM liquid, and those that displayed abnormal swimming in the first 5 min were selected. Mutant alleles were outcrossed four times. Cloning of *unc-80* and gfp-promotor fusion experiments are detailed in *SI Materials and Methods*.

ACKNOWLEDGMENTS. We thank K. Schuske, M. Ailion, E. Jorgensen, M. Zhen, M. Sedensky, and P. Morgan for sharing unpublished data; anonymous reviewers for advice; C. Hsu and R. Lanam for assistance; M. Zimmer, J. Dantzker, and T. Yu for help with imaging; N. Chronis for constructing image chamber; M. Chklovskii for help with analysis of calcium imaging data; D. Parry for help with mapping; and McIntire and Lockery labs for criticism. Strains were provided by C. Bargmann, S. Mitani, T. Stiernagle, and the *Caenorhabditis* Genetics Center. This work was supported by a National Research Service Award fellowship from the National Institutes of Health (NIH) (J.T.P.), an Arnold and Mabel Beckmann Graduate Student Fellowship of the Watson School of Biological Sciences (B.L.C.), and an R01 grant from NIH (S.L.M.).

1. Feldman JL, Mitchell GS, Nattie EE (2003) Breathing: rhythmicity, plasticity, chemosensitivity. *Annu Rev Neurosci* 26:239–266.
2. Jing J, *et al.* (2007) From hunger to satiety: reconfiguration of a feeding network by Aplysia neuropeptide Y. *J Neurosci* 27:3490–3502.
3. Nusbaum MP, Beenhakker MP (2002) A small-systems approach to motor pattern generation. *Nature* 417:343–350.
4. Marder E, Bucher D (2001) Central pattern generators and the control of rhythmic movements. *Curr Biol* 11:R986–R996.
5. Marder E, Calabrese RL (1996) Principles of rhythmic motor pattern generation. *Physiol Rev* 76:687–717.
6. Paton JF, Abdala AP, Koizumi H, Smith JC, St John WM (2006) Respiratory rhythm generation during gasping depends on persistent sodium current. *Nat Neurosci* 9:311–313.
7. Kiehn O (2006) Locomotor circuits in the mammalian spinal cord. *Annu Rev Neurosci* 29:279–306.
8. Lanuza GM, Gosgnach S, Pierani A, Jessell TM, Goulding M (2004) Genetic identification of spinal interneurons that coordinate left-right locomotor activity necessary for walking movements. *Neuron* 42:375–386.
9. Brenner S (1974) The genetics of *Caenorhabditis elegans. Genetics* 77:71–94.
10. de Bono M, Maricq AV (2005) Neuronal substrates of complex behaviors in *C. elegans. Annu Rev Neurosci* 28:451–501.
11. Korta J, Clark DA, Gabel CV, Mahadevan L, Samuel ADT (2007) Mechanosensation and mechanical load modulate the locomotory gait of swimming *C. elegans. J Exp Bio* 210:2383–2389.
12. Caswell-Chen EP, *et al.* (2005) Revising the standard wisdom of *C. elegans* natural history: ecology of longevity. *Sci Aging Knowledge Environ* 40:30.
13. Humphrey JA, *et al.* (2007) A putative cation channel and its novel regulator: cross-species conservation of effects on general anesthesia. *Curr Biol* 17:624–629.
14. Lu B, *et al.* (2007) The neuronal channel NALCN contributes resting sodium permeability and is required for normal respiratory rhythm. *Cell* 129:371–383.
15. Jospin M, *et al.* (2007) UNC-80 and the NCA ion channels contribute to endocytosis defects in synaptojanin mutants. *Curr Biol* 17:1595–1600.
16. Yeh E, *et al.* A Putative cation channel, NCA-1, and a novel protein, UNC-80, transmit neuronal activity in *C. elegans. PLoS Biol* 6:e55, 2008.
17. Wicks SR, de Vries CJ, van Luenen HG, Plasterk RH (2000) CHE-3, a cytosolic dynein heavy chain, is required for sensory cilia structure and function in *Caenorhabditis elegans. Dev Biol* 221:295–307.
18. Morgan PG, Cascorbi HF (1985) Effect of anesthetics and a convulsant on normal and mutant *Caenorhabditis elegans. Anesthesiology* 62:738–744.
19. Schultz J, *et al.* (1998) SMART, a simple modular architecture research tool: identification of signaling domains. *Proc Natl Acad Sci USA* 95:5857–5864.
20. Groves MR, Barford D (1999) Topological characteristics of helical repeat proteins. *Curr Opin Struct Biol* 9:383–389.
21. Harris TW, Hartwieg E, Horvitz HR, Jorgensen EM (2000) Mutations in synaptojanin disrupt synaptic vesicle recycling. *J Cell Biol* 150:589–600.
22. Schafer WR, Kenyon CJ (1995) A calcium-channel homologue required for adaptation to dopamine and serotonin in *Caenorhabditis elegans. Nature* 375:73–78.
23. Lee RY, Lobel L, Hengartner M, Horvitz HR, Avery L (1997) Mutations in the alpha1 subunit of an L-type voltage-activated Ca^{2+} channel cause myotonia in *Caenorhabditis elegans. EMBO J* 16:6066–6076.
24. Shtonda B, Avery L (2005) CCA-1, EGL-19 and EXP-2 currents shape action potentials in the *Caenorhabditis elegans* pharynx. *J Exp Biol* 208:2177–2190.
25. Esch T, Mesce KA, Kristan WB (2002) Evidence for sequential decision making in the medicinal leech. *J Neurosci* 22:11045–11054.
26. Briggman KL, Abarbanel HD, Kristan WB Jr (2005) Optical imaging of neuronal populations during decision-making. *Science* 307:896–901.
27. Nakayama M, Iida M, Koseki H, Ohara O (2006) A gene-targeting approach for functional characterization of KIAA genes encoding extremely large proteins. *FASEB J* 20:718–1720.
28. Lein ES, *et al.* (2007) Genome-wide atlas of gene expression in the adult mouse brain. *Nature* 445:168–176.
29. Locascio A, Vega S, de Frutos CA, Manzanares M, Nieto MA (2002) Biological potential of a functional human SNAIL retrogene. *J Biol Chem* 277:38803–38809.
30. Talavera K, Nilius B (2006) Biophysics and structure-function relationship of T-type Ca^{2+} channels. *Cell Calcium* 40:97–114.
31. Kwiecien R, *et al.* (1998) Endogenous pacemaker activity of rat tumour somatotrophs. *J Physiol* 508:883–905.
32. Irisawa H, Brown HF, Giles W (1993) Cardiac pacemaking in the sinoatrial node. *Physiol Rev* 73:197–227.